Combustion Science and Technology
Publication details, including instructions for authors and subscription information:
http://www.informaworld.com/smpp/title~content=t713456315

Edge-Flames and Their Stability

J. Buckmaster[a]
[a] Department of Aeronautical and Astronautical Engineering, University of Illinois, Urbana, IL

To cite this Article Buckmaster, J.(1996) 'Edge-Flames and Their Stability', Combustion Science and Technology, 115: 1, 41 — 68
To link to this Article: DOI: 10.1080/00102209608935522
URL: http://dx.doi.org/10.1080/00102209608935522

Combust. Sci. Tech., 1996, Vol. 115, pp. 41–68
Reprints available directly from the publisher
Photocopying permitted by license only

Edge-Flames and Their Stability

J. BUCKMASTER

Department of Aeronautical and Astronautical Engineering,
University of Illinois, Urbana, IL 61801

(Received 2 August 1995; in final form 20 February 1996)

Flame sheets that arise in non-premixed combustion often have edges. The leading edge of a flame spreading over a fuel-bed, solid or liquid, is one example. The edge of a hemi-spherical candle flame in microgravity is another. We construct a one-dimensional model which contains some of the essential physics of these edge-flames, and use this model to describe stationary solutions and their stability. The model corresponds to a new class of combustion waves which resemble deflagrations in some respects yet exhibit important differences. Thus, in a uniform flow, wave-like solutions are possible with positive, negative or vanishing wave-speeds, depending on an assignable Damköhler number. At large activation energy, reaction is concentrated primarily in a thin region (the edge) but it persists, in diminished form, behind the edge. This residual reaction plays a key role in defining the flame - or edge-temperature which, in turn, controls the dynamics of the structure. The familiar Lewis-number stability boundaries of deflagrations are present in modified form and provide tentative explanations of pulsations and cellular structures that have been observed experimentally.

LIST OF SYMBOLS

$B, \bar{B}$	Pre-exponential factor
$C_i \;\; i = 1,2,3$	coefficients of side-terms
C_{3_2}	ε coefficient in expansion of C_3
C_p	specific heat
D	Damköhler number
D_1	εD
D_X	oxygen diffusion coefficient
D_Y	fuel diffusion coefficient
E	activation energy
h	flame-edge location
H	$h/\sqrt{\varepsilon}$

J	$(C_p T_a/Q)\Phi + Z$
k	wave-number
l	(Le-1)/ε
L	transverse length scale
Le_Y	fuel Lewis number
M	transverse mass flux
Q	heat of reaction
R	gas constant
s	z/L
t	time
T	temperature
T_a	Burke-Schumann flame temperature
U	edge speed
V	non-dimensional edge speed
x	transverse distance
X	oxygen mass fraction
X_a	equilibrium X when $T = T_a$
X_i	coefficient functions in X-expansion in flame edge
y	distance parallel to edge
Y	fuel mass fraction
Y_a	equilibrium Y when $T = T_a$
Y_i	coefficient functions in Y-expansion in flame edge
z	distance along flame
Z	fuel mass fraction outside of the flame edge
Z_i	coefficient functions in Z-expansion
α_1	Eq. (36)
β_1, β_2	Eqs. (61b), (67b)
γ_X, γ_Y	stoichiometric coefficients
ε	RT_a/E
θ	T/T_a
θ_i	coefficient functions in θ-expansion in flame edge
λ	heat conduction coefficient
ξ	distance in flame-edge
ρ	density
σ	s-h
τ	non-dimensional time
ϕ	Eq. (15)
Φ	θ outside of the flame-edge
Φ_i	coefficient functions in Φ-expansion

Ψ	$(C_p T_a/Q)(\theta - \theta_w) + (Y - Y_w)$
$\Omega, \bar{\Omega}$	reaction rate
$()_i$	expansion coefficients
$()_s$	steady state
$()_w$	supply values
$()'$	unsteady perturbations
$()^-$	values to the left of the flame-edge

INTRODUCTION

Edge-flames are a common characteristic of non-premixed combustion. For example, a flame propagating over a fuel-bed will have a leading edge standing some distance above the bed (Fig. 1). A candle burning in microgravity will have a hemispherical shape with a well-defined circular edge (Fig. 2), Dietrich,

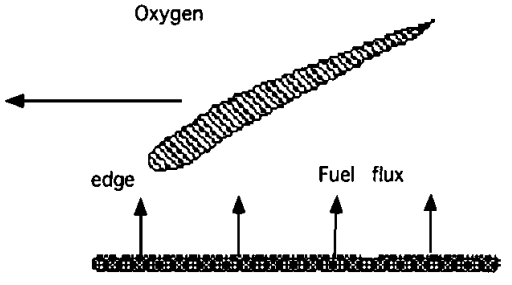

FIGURE 1 Flame spreading over a fuel bed.

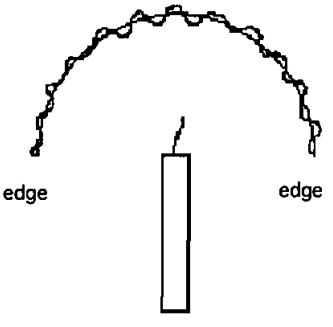

FIGURE 2 Hemi-spherical candle flame under microgravity conditions.

Ross, and T'ien (1994). And a turbulent diffusion flame will have a hole ripped in it where the local scalar dissipation rate is large enough, and this hole will have an edge.

Edge-flame dynamics is an important subject. Thus in the turbulent context we would like to know what conditions will cause the hole to expand, what conditions will cause it to shrink, and whether or not there are meaningful conditions under which the hole will do neither, Dold *et al.* (1991), §4.

Systematic experimental studies of edge-flames have not been carried out, but there have been observations that are relevant to our study, and we shall refer to three.

Dietrich *et al.* (1994) have observed candle flames in microgravity which extinguish after some period due to asphyxiation. Large scale oscillations occur prior to extinction, with the leading edge moving over the hemispherical surface defined by the steadily-burning flame so that the solid angle subtended by the flame at the sphere center oscillates between a value close to 2π and a much smaller value. Note that the heavy hydrocarbons that fuel a candle flame will define a Lewis number that is significantly greater than 1.

Chan and T'ien (1978) have examined flames in a Kirkby-Schmitz apparatus, but with the fuel (ethanol and other choices) supplied as vapor from an evaporating pool. The flame is a circular disk confined within a circular tube with a gap between the disk edge and the tube surface. Prior to extinction, oscillations are observed in which the disk expands and shrinks in a symmetric fashion, so that the distance between the flame edge and the tube wall oscillates. An ethanol flame will have an effective Lewis number greater than 1.

Chen, Bradley, and Ronney (1992) have examined burner flames in a variety of atmospheres. When the atmosphere is chosen so that the effective Lewis number is small, cellular flame structures are observed.

The oscillations observed in the first two studies for Lewis numbers greater than 1, and the cellular structures observed in the third for Lewis numbers less than 1, bring to mind the familiar stability boundaries of deflagrations (e.g. Buckmaster and Ludford (1983)). But although a significant degree of mixing occurs at the edges of edge-flames, they are not deflagrations. And, of course, they are not diffusion flames. They are something in between, a hybrid, and our purpose here is to construct a simple model which contains some of the essential characteristics of this hybrid structure. This model admits wave-like solutions in which the edge advances, retreats, or stands still, and we shall discuss the stability of these solutions for the special case when the Lewis number of the oxidizer is 1, but that of the fuel differs from 1. The asymptotic structures valid in the limit of infinite activation energy have features familiar

from deflagration studies, but, as we shall see, there are crucial, if subtle, differences. One consequence is that the familiar closure problem for stability studies is resolved in a novel fashion that only resembles a NEF strategy (Near-Equidiffusional Flames, Buckmaster and Ludford (1983), p. 52) for deflagrations.

One-Dimensional Model of an Edge-Flame

A cartoon which identifies key features of our model is shown in Figure 3. This looks like a flame in a channel, but it should not be interpreted in such a literal fashion. It is simply a device to display some important characteristics. Amongst other things, it does not show any flame-structures at the edge that can arise from mixing to the left of the edge (see, for example, Kioni *et al.* (1993)).

The flame is affected by two boundaries, as is always the case in non-premixed combustion. One boundary is the oxygen-supply boundary at which the characteristic value of the oxygen concentration is X_w. This would be located at infinity for the candle flame, at the upper end of the tube for the Kirkby-Schmitz apparatus.

The second boundary, on the other side of the flame, is the fuel-supply boundary, where the characteristic value of the fuel concentration is Y_w. It corresponds to the wick for the candle flame, the pool for the Kirby-Schmitz apparatus.

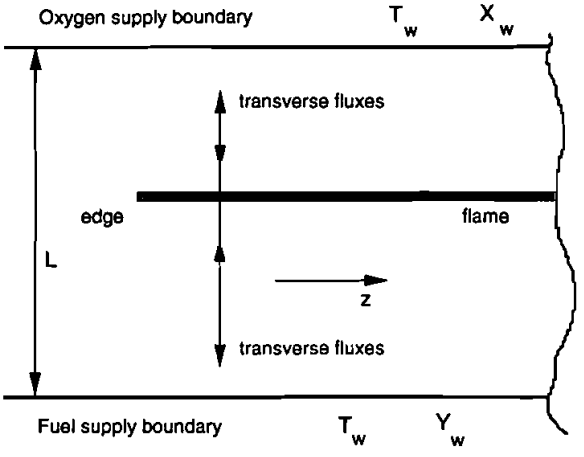

FIGURE 3 Cartoon of the edge-flame model.

The combustion field is assumed to have a charactreistic length scale L in the direction perpendicular to the flame. An appropriate choice for L for the candle flame would be the flame radius, for example.

Each boundary will have a characteristic temperature and, for simplicity, we shall adopt the single value T_w. T_w will usually be much smaller than the flame temperature, so that this not an important point.

Finally, we assume that there is no applied flow over the edge (in the z-direction) in the adopted frame, but transverse flow is not ruled out. The edge itself can move in the z-direction.

With this scenario in mind, let us examine typical model equations governing the combustion field in a Cartesian coordinate system. These are:

$$\rho C_p \frac{\partial T}{\partial t} - \lambda \frac{\partial^2 T}{\partial z^2} = \left\{ \lambda \frac{\partial^2 T}{\partial x^2} - C_p M \frac{\partial T}{\partial x} \right\}_T + Q\Omega, \tag{1a}$$

$$\rho \frac{\partial X}{\partial t} - \rho D_x \frac{\partial^2 X}{\partial z^2} = \left\{ \rho D_X \frac{\partial^2 X}{\partial x^2} - M \frac{\partial X}{\partial x} \right\}_X - \gamma_X \Omega, \tag{1b}$$

$$\rho \frac{\partial Y}{\partial t} - \rho D_Y \frac{\partial^2 Y}{\partial z^2} = \left\{ \rho D_Y \frac{\partial^2 Y}{\partial x^2} - M \frac{\partial Y}{\partial x} \right\}_Y - \gamma_Y \Omega. \tag{1c}$$

Note that the terms which correspond to transverse fluxes—the 'side-terms'—have been enclosed in brackets. Ω is the reaction term, but we are not ready to define it at this moment.

We now simplify the side-terms by replacing them in the following fashion:

$$\{\}_T \to -\lambda \frac{(T - T_w)}{L^2} C_1, \tag{2a}$$

$$\{\}_X \to \rho D_X \frac{(X_w - X)}{L^2} C_2, \tag{2b}$$

$$\{\}_Y \to \rho D_Y \frac{(Y_w - Y)}{L^2} C_3. \tag{2c}$$

The essential ideal is that the key physical contribution of the side terms is heat loss to the boundaries ($T > T_w$), oxygen gain from the oxygen boundary ($X_w > X$), and fuel gain from the fuel boundary ($Y_w > Y$).

This is a bold move (or crude, depending on ones point of view) but is not novel. An example which is closer to the spirit of our investigation than any other is afforded by the work of Weber, Mercer, Gray, and Watt (1995) on a two-dimensional reactive thermal problem which is reduced to a one-dimensional problem. An earlier example is the one-dimensional heat loss analysis of Spalding (1957) for a flame in a tube.

There is no *a priori* assumption that the side terms are small. Although it might seem that a large heat loss (via the term in C_1) would quench the flame, this effect is negated by large fluxes of reactants via the C_2, C_3 terms.

C_1,C_2, and C_3 are constants, but since C_1 can be scaled out, viz.

$$z \to \frac{z}{\sqrt{C_1}}, t \to \frac{t}{C_1}, \Omega \to \Omega C_1, C_2 \to C_1 C_2, C_3 \to C_1 C_3, \tag{3}$$

we may, without loss of generality (*wlog*), take it to be 1.

Equilibrium

Equilibrium is defined by the constant solutions of Eqs. (1), (2) ($\partial/\partial t = \partial/\partial z = 0$). It corresponds to a balance between the side terms and the reaction. It follows, because of the linear nature of Eqs. (2), that, in equilibrium, X and Y are linear functions of T ($C_1\lambda(T_e - T_w)/Q = C_2 \rho D_X (X_w - X_e)/\gamma_X = C_3 \rho D_Y (Y_w - Y_e)/\gamma_Y$). We define T_a as the Burke-Schumann flame temperature for the underlying diffusion-flame system. In other words T_a is the flame temperature of the equilibrium state when the Damköhler number equals infinity. We then define X_a and Y_a by

$$X_a = X_e(T_a), \quad Y_a = Y_e(T_a) \tag{4}$$

where X_e and Y_e are the linear equilibrium functions.

With these definitions, the reactions rate is chosen to be

$$\Omega = B(X - X_a)(Y - Y_a)e^{-E/RT}, \tag{5}$$

the second defining ingredient of our model.

There are several points to be made in connection with the formula (5). Note that, following the substitutions (2), X and Y are *representative* or *average* values of the concentrations so that (5) is a resolution of the closure problem

for the reaction rate. Also, for large activation energy, reaction will only be significant for values of T close to T_a, and the true concentrations in the neighborhood of the reaction zone will be small, vanishing in the limit of infinite Damköhler number, so that it is natural to associate $(X - X_a)$ and $(Y - Y_a)$ with these local concentrations. Clearly related to this is the fact that, with the choice (5), we guarantee that equilibrium for infinite Damköhler number (essentially $B \to \infty$) is characterized by $T \to T_a$.

Non-Dimensional Equations

Consider a stationary structure that propagates with speed U to the left (Fig. 3) so that in a frame attached to the edge, $\partial/\partial t \to U\,\partial/\partial z$. We introduce non-dimensional variables by the formulas

$$s = \frac{z}{L}, \theta = \frac{T}{T_a}, V = \frac{\rho C_p L}{\lambda} U, \bar{\Omega} = \frac{C_p L^2}{\lambda}\Omega, \tag{6a,b,c,d}$$

$$\bar{B} = \frac{C_p L^2}{\lambda} e^{-1/\varepsilon} B, \varepsilon = \frac{R T_a}{E}, \tag{6e,f}$$

so that the governing equations become

$$V\frac{d\theta}{ds} - \frac{d^2\theta}{ds^2} = -(\theta - \theta_w) + \frac{Q}{C_p T_a}\bar{\Omega}, \tag{7a}$$

$$V\frac{dX}{ds} - \frac{d^2X}{ds^2} = C_2(X_w - X) - [\gamma_X]\bar{\Omega}, \tag{7b}$$

$$Le_Y V\frac{dY}{ds} - \frac{d^2Y}{ds^2} = C_3(Y_w - Y) - [\gamma_Y Le_Y]\bar{\Omega}, \tag{7c}$$

$$\bar{\Omega} = \bar{B}(X - X_a)(Y - Y_a)e^{(1 - 1/\theta)/\varepsilon}. \tag{7d}$$

Note that γ_X can be scaled out, viz.

$$X \to \gamma_X X, X_w \to \gamma_X X_w, X_a \to \gamma_X X_a, \bar{B}\gamma_X \to \bar{B}, \tag{8}$$

and the factor γ_Y Le_Y in Eq. (7c)may be similarly eliminated, so that *wlog* each factor in square brackets in (7b) and (7c) can be replaced by 1.

We have taken the Lewis number for X to be 1 in this first study, but Le_Y is different from 1 in anticipation that this will lead to non-trivial stability results.

It turns out that solutions to Eqs. (7) not only determine the edge-speed V but, in addition, determine the coefficients C_2 and C_3. This is a global stoichiometric balance requirement and a global energy balance requirement. In the present case

$$C_2 = 1 \tag{9}$$

so that there is a Schvab-Zeldovich relationship

$$X - X_w = -\frac{C_p T_a}{Q}(\theta - \theta_w). \tag{10}$$

As we shall see, when Le_Y is different from 1, so is C_3.

To put our problem in the context of a well-understood mathematical framework, note that if $Le_Y = 1$, $C_3 = 1$, and the Schvab-Zeldovich relation (10) is also satisfied by Y, θ, the problem reduces to one for θ alone, viz.,

$$V\frac{d\theta}{ds} - \frac{d^2\theta}{ds^2} = f(\theta), \tag{11}$$

$$f(\theta) = -(\theta - \theta_w) + \frac{C_p T_a}{Q}\bar{B}(\theta_a - \theta)^2 e^{(1-1/\theta)/\varepsilon}.$$

For certain choices of $\bar{B}$, the function f has three simple zeros (Fig. 4), and reaction-diffusion equations of this type are routinely discussed in the mathematics literature (e.g. Grindrod (1991)).

Equilibrium Revisited

The equations of equilibrium are

$$\bar{\Omega} = \frac{C_p T_a}{Q}(\theta - \theta_w) = (X_w - X) = C_3(Y_w - Y), \tag{12}$$

so that

$$\frac{C_p T_a}{Q}(1 - \theta_w) = (X_w - X_a) = C_3(Y_w - Y_a) \tag{13}$$

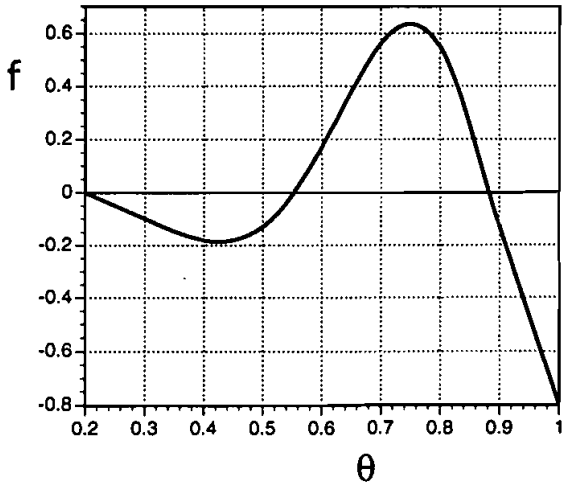

FIGURE 4 The function f (cf. Grindrod (1991), Fig. 1. 7.).

by the definition of X_a and Y_a. When X and Y are eliminated, Eqs. (12) are equivalent to

$$(1-\theta)^2 e^{(1-1/\theta)/\varepsilon} = \frac{C_3}{\bar{B}} \cdot \frac{Q}{C_p T_a}(\theta - \theta_w) \tag{14}$$

The left side of this equation is sketched in Figure 5 together with the right side for three different values of the coefficient $\sim \bar{B}^{-1}$. When $\bar{B}$ is small there is a single solution close to θ_w. For larger values of $\bar{B}$ there are three solutions, one close to θ_w, one close to 1, and one that has an intermediate value. For even larger values of $\bar{B}$ there is, again, only one solution, close to 1. Then if we plot variations of equilibrium values of θ with the Damköhler number ($\sim \bar{B}$) we obtain an S-shaped response (Fig. 6). This a familiar characteristic of diffusion flames.

The description of the equilibrium solutions can be simplified in the asymptotic limit $\varepsilon \to 0$ (large activation-energy asymptotics). On the top banch we write

$$\theta = 1 - \varepsilon \phi \tag{15}$$

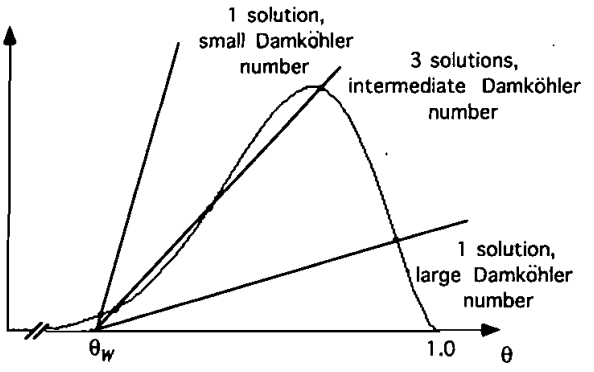

FIGURE 5 Equilibrium solutions. The curve is the left side of Eq. 14, the straight lines are the right side for different values of $\bar{B}$.

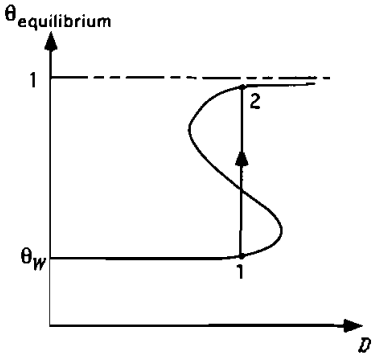

FIGURE 6 The S-shpaed equilibrium response. We are concerned with solutions which correspond to 1: $z = -\infty$; 2: $z = +\infty$.

whence

$$\phi^2 e^{-\phi} = \frac{1}{D}, D = \frac{\varepsilon^2 \bar{B}}{C_3} \cdot \frac{C_p T_a}{Q} \cdot \frac{1}{1-\theta_w}. \tag{16a,b}$$

The left side of Eq. (16a) has a maximum value of $4\, e^{-2}$ when $\phi = 2$ so that there is no solution if $D < e^2/4$. When $D > e^2/4$ the top branch corresponds to the smallest of the two possible values of ϕ. We are concerned with $O(1/\varepsilon)$

values of D (then $V = O(1)$, as we shall see), viz.

$$D = \frac{1}{\varepsilon} D_1, \quad D_1 = \frac{\varepsilon^3 \bar{B}}{C_3} \cdot \frac{C_p T_a}{Q} \cdot \frac{1}{1-\theta_w} = O(1) \tag{17}$$

so that

$$\phi \sim \sqrt{\varepsilon / D_1} \tag{18}$$

and the top-branch equilibrium corresponds to

$$\theta \sim 1 - \frac{\varepsilon \sqrt{\varepsilon}}{\sqrt{D_1}} + \cdots, \tag{19a}$$

$$Y \sim Y_a + \frac{1}{C_3} \cdot \frac{C_p T_a}{Q} \cdot \frac{\varepsilon \sqrt{\varepsilon}}{\sqrt{D_1}} + \ldots. \tag{19b}$$

On the bottom branch the reaction is exponentially small, so that

$$\theta \sim \theta_w, X \sim X_w, Y \sim Y_w. \tag{20}$$

We are concerned with solutions of Eqs. (7) which describe a transition from the bottom branch of the S-response to the top branch. That is, state (1) in Figure 6 describes the conditions at $s \to -\infty$ (Eq. (20)), and state (2) describes the conditions at $s \to +\infty$ (Eqs. (19)).

Note that when Eqn. (11)is valid, a single integration yields the formula

$$V = \frac{\int_1^2 f(\theta)\, d\theta}{\int_{-\infty}^{\infty} ds\, (d\theta/ds)^2}, \tag{21}$$

and the sign of $V$is defined by the numerator. The function f vanishes on the S-curve of Figure 6 and is negative between the point 1 and intersection of the line 1-2 with the middle branch, positive between the intersection and point 2. Thus, if point 2 is close to the static quenching point ($D = e^2/4$), the negative contribution to the integral dominates and Vwill be negative; if the point 1 is close to the static ignition point, the positive contribution dominates and V will be positive. There is a critical Damköhler number for which $V = 0$.

Stationary Structure in the Limit $\varepsilon \to 0$

The stationary structure is sketched in Figure 7 and has many similarities with the large activation energy structure of the classical deflagration. In the region $s<0$ the temperature θ is less than 1 and reaction is frozen. In a thin region located at $s\sim 0$ there is intense reaction balanced by diffusion. In deflagrations this is called the flame-sheet, but here it is appropriate to call it the flame-edge. In the region $s>0$ there is reaction balancing the side-terms, but the reaction is smaller by a factor ε than that within the flame-edge. It is natural to associate the enhanced reaction at the edge with the premixed burning that occurs at the edge in the underlying two-dimensional structure.

Flame-Edge Analysis

To analyze the flame-edge we seek a solution in the form

$$\theta \sim 1 + \varepsilon \theta_2(\xi) + O(\varepsilon\sqrt{\varepsilon}), \tag{22a}$$

$$X \sim X_a + \varepsilon X_2 + O(\varepsilon\sqrt{\varepsilon}), \tag{22b}$$

$$Y \sim Y_a + \varepsilon Y_2(\xi) + O(\varepsilon\sqrt{\varepsilon}), \quad \xi = s/\varepsilon \tag{22c,d}$$

Thus

$$\frac{-C_p T_a}{Q}\frac{d^2\theta_2}{d\xi^2} = \varepsilon^3 \bar{B} X_2 Y_2 e^{\theta_2} = \frac{d^2 X_2}{d\xi^2} = \frac{d^2 Y_2}{d\xi^2}. \tag{23}$$

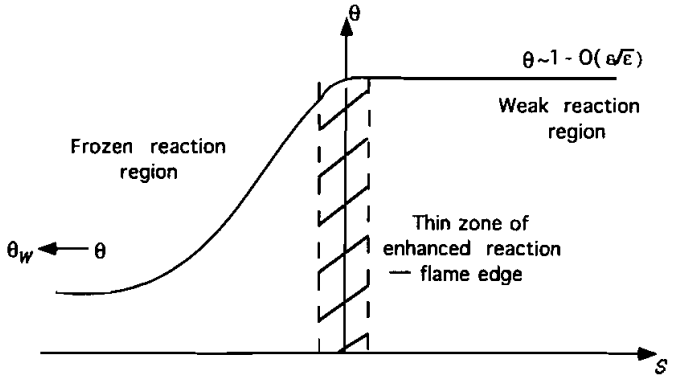

FIGURE 7 Steady-state temperature distribution.

Note that this system makes sense if $\varepsilon^3 \bar{B}$ is $O(1)$, as anticipated by Eq. (17b).

There are no $O(1)$ gradients in the region $s>0$, so that

$$\theta_2, X_2, Y_2 \to \theta_{2_R}, X_{2_R}, Y_{2_R} \quad \text{as } \xi \to +\infty. \tag{24}$$

Thus

$$Y_2 - Y_{2_R} = -\frac{C_p T_a}{Q}(\theta_2 - \theta_{2_R}), \quad X_2 = -\frac{C_p T_a}{Q}\theta_2, \tag{25a, b}$$

and

$$\frac{d^2\theta_2}{d\xi^2} = \varepsilon^3 \bar{B}\theta_2\left[Y_{2_R} - \frac{C_p T_a}{Q}(\theta_2 - \theta_{2_R})\right]e^{\theta_2}. \tag{26}$$

When Eq. (26) is integrated once we deduce the condition

$$\underline{\xi \to -\infty} \quad \frac{1}{2}\left(\frac{d\theta_2}{d\xi}\right)^2 \to \varepsilon^3 \bar{B}\, Y_{2_R}(1-\theta_{2_R})e^{\theta_{2R}} + \varepsilon \bar{B}\frac{C_p T_a}{Q}(2-\theta_{2_R})e^{\theta_{2R}}. \tag{27}$$

However, there can be no $O(\varepsilon)$ perturbations in the region behind the flame-edge ($s>0$),
i.e.

$$\theta_{2_R} = Y_{2_R} = 0 \tag{28}$$

so that Eq. (27) becomes

$$\underline{\xi \to -\infty} \quad \frac{d\theta_2}{d\xi} \to 2\sqrt{\frac{C_p T_a}{Q}\varepsilon^3 \bar{B}}. \tag{29}$$

The condition (28) follows from the fact that $\bar{\Omega}$ can be at most $O(1)$ in $s>0$ if it is to be balanced, so that

$$(X - X_a)(Y - Y_a) = O(\varepsilon^3) \quad \text{in } s>0, \tag{30}$$

and each factor can be no smaller than $O(\varepsilon\sqrt{\varepsilon})$ because of the condition (19).

The gradient (29) is to be matched with the gradient in the preheat zone, to which we now turn our attention.

Solution in s > 0

In this region reaction is negligible so that T and Y are governed by the equations

$$V\frac{d\theta}{ds}-\frac{d^2\theta}{ds^2}+(\theta-\theta_w)=0, \tag{31a}$$

$$Le_Y V\frac{dY}{ds}-\frac{d^2Y}{ds^2}+C_3(Y-Y_w)=0. \tag{31b}$$

We make the choice

$$Le_Y=1+\varepsilon l, \quad l=O(1) \tag{32}$$

(cf. NEFs, Buckmaster and Ludford, *loc. cit.*) in order to carry out a stability analysis. And then, as we shall see, it is appropriate to write

$$C_3=1+\varepsilon C_{3_2}+\cdots. \tag{33}$$

Solutions to Eqs. (31)are sought in the form

$$\theta=\Phi_0^-+\varepsilon\Phi_2^-+O(\varepsilon\sqrt{\varepsilon}), \tag{34a}$$

$$Y=Z_0^-+\varepsilon Z_2^-+O(\varepsilon\sqrt{\varepsilon}), \tag{34b}$$

whence

$$\Phi_0^-=\theta_w+(1-\theta_w)e^{\alpha_1 s}, \tag{35a}$$

$$\Phi_2^-=\theta_{2L}e^{\alpha_1 s}, \tag{35b}$$

where

$$\alpha_1=\frac{1}{2}(V+\sqrt{V^2+4}) \tag{36}$$

and, within the flame-edge,

$$\theta_2\to(1-\theta_w)\alpha_1\xi+\theta_{2_L} \quad \text{as } \xi\to-\infty. \tag{37}$$

Z_0^- is given by the formula

$$Z_0^- = Y_w + (Y_a - Y_w)e^{\alpha_1 s}, \tag{38}$$

and we do not describe Z_2^- since it is contained within the discussion of the next sub-section.

The matching condition (37), when combined with (29), leads to the formula

$$\frac{4}{(1-\theta_w)}\sqrt{\frac{C_p T_a}{Q}\varepsilon^3 \bar{B}} = V + \sqrt{V^2+4} \tag{39}$$

which determines the edge-speed V. The left side essentially varies from 0 to ∞ as the Damköhler number ranges over values between the two turning points of Figure 6. And the right side varies over the same interval as V ranges from $-\infty$ to $+\infty$. For, as $V \to \infty$,

$$V + \sqrt{V^2+4} \sim -\frac{2}{V}, \tag{40}$$

and as $V \to \infty$,

$$V + \sqrt{V^2+4} \sim 2V. \tag{41}$$

Both positive and negative edge speeds are possible, depending upon the Damköhler number, and there is a stationary edge when

$$\frac{2}{(1-\theta_w)}\sqrt{\frac{C_p T_a}{Q}\varepsilon^3 \bar{B}} = 1. \tag{42}$$

Calculation of C_3.

It was noter earlier that C_3 cannot be arbitrarily assigned, but must be chosen to satisfy global stoichiometry. C_{3_2} (cf. Eqn. (32)) must be determined before we can proceed with a stability analysis.

If $\bar{\Omega}$ is eliminated between Eqs. (7a) and (7c) we deduce the equation

$$V\frac{d}{ds}\left(\frac{C_p T_a}{Q}\theta\right) + Le_Y V\frac{dY}{ds} - \frac{d^2}{ds^2}\left(\frac{C_p T_a}{Q}\theta\right) - \frac{d^2 Y}{ds^2} = \frac{C_p T_a}{Q}(\theta_w - \theta) + C_3(Y_w - Y). \tag{43}$$

Using the formulas (32), (33) and defining

$$\Psi = \frac{C_p T_a}{Q}(\theta - \theta_w) + (Y - Y_w), \tag{44}$$

Eq. (43) is equivalent to

$$V\frac{d\Psi}{ds} - \frac{d^2\Psi}{ds^2} + \Psi = \varepsilon C_{3_2}(Y_w - Y) - \varepsilon l V\frac{dY}{ds} + o(\varepsilon). \tag{45}$$

Boundary conditions are

$$\underline{s \to -\infty} \quad \Psi \to O. \tag{46a}$$

$$\underline{s \to +\infty} \quad \Psi \to \frac{C_p T_a}{Q}(1 - \theta_w) + (Y_a - Y_w) + O(\varepsilon\sqrt{\varepsilon})$$

$$= \varepsilon\frac{C_p T_a}{Q}(1 - \theta_w) C_{3_2} + o(\varepsilon). \tag{46b}$$

Thus

$$\Psi = \varepsilon\Psi_2 + \cdots \tag{47}$$

where

$$V\frac{d\Psi_2}{ds} - \frac{d^2\Psi_2}{ds^2} + \Psi_2 = C_{3_2}(Y_w - Y) - lV\frac{dY}{ds} \tag{48}$$

with

$$\Psi_2 \to 0 \text{ as } s \to -\infty, \quad \Psi_2 \to \frac{C_p T_a}{Q}(1 - \theta_w) C_{3_2} \text{ as } s \to +\infty, \tag{49a,b}$$

and the right side of Eq. (48) is to be prescribed to first order only.

If Eq. (48) is examined on the scale $s = O(1)$, the right side is discontinuous at $s = 0$ but Ψ_2 and $d\Psi_2/ds$ are continuous. Thus a unique solution is readily constructed. But Ψ_2 must be constant in $s > 0$,

$$\text{i.e.} \quad \Psi_2 = \frac{C_p T_a}{Q}(1-\theta_w) C_{3_2} \text{ in } s>0 \tag{50}$$

to eliminate $O(\varepsilon)$ perturbations of $(X - X_a)$ and $(Y - Y_a)$ (cf. Eq. (30)) and in this way a constraint on C_{3_2} is defined. Thus

$$\Psi_2 = C_{3_2}\frac{C_p T_a}{Q}(1-\theta_w)e^{\alpha_1 s} + \frac{(Y_w - Y_a)(C_{3_2} + lV\alpha_1)}{(V-2\alpha_1)} s e^{\alpha_1 s}, s<0 \tag{51}$$

and

$$C_{3_2} = \frac{2lV}{V+\sqrt{V^2+4}}. \tag{52}$$

Note that with Φ_2, Ψ_2 determined, Z_2^- is known.

Unsteady Perturbations—the Stability Analysis

We now turn to the stability analysis. Here we confront the closure problem that always arises in large activation energy studies. Thus it is natural, in view of the steady solution, to examine $O(\varepsilon\sqrt{\varepsilon})$ perturbations in the region behind the flame-edge, corresponding to $O(\varepsilon\sqrt{\varepsilon})$ perturbations of the temperature at the edge itself. Because of the Arrhenius kinetics the corresponding variations in the edge speed are $O(\sqrt{\varepsilon})$, so that the perturbations ahead of the edge are also $O(\sqrt{\varepsilon})$. But overall connections within the combustion field, global energy conservation and the like, imply, in general, that $O(\sqrt{\varepsilon})$ perturbations ahead of the edge will be associated with $O(\sqrt{\varepsilon})$ perturbations behind the edge, and a contradiction is reached. The key to a rational asymptotic treatment is to identify circumstances for which $O(\sqrt{\varepsilon})$ perturbations are not generated behind the edge. Thus the analogous dilemma in deflagrations can be resolved within the context of NEFs. Here the resolution comes from the choice (32) (as with NEFs) together with restrictions on the class of permissible disturbances. Instability for a restricted class of disturbances is instability, not withstanding.

The governing equations are

$$\frac{\partial\theta}{\partial\tau}+V\frac{\partial\theta}{\partial s}-\frac{\partial^2\theta}{\partial s^2}-\frac{\partial^2\theta}{\partial y^2}=(\theta_w-\theta)+\frac{Q}{C_pT_a}\bar{\Omega}, \tag{53a}$$

$$(1+\varepsilon l)\frac{\partial Y}{\partial\tau}+(1+\varepsilon l)V\frac{\partial Y}{\partial s}-\frac{\partial^2 Y}{\partial s^2}-\frac{\partial^2 Y}{\partial y^2}=(1+\varepsilon C_{3_2})(Y_w-Y)-\bar{\Omega}, \tag{53b}$$

which differ from Eqs. (7) by the addition of time derivatives and diffusion in the y-direction, measured parallel to the edge.

Suppose the disturbed flame-sheet is located at

$$s=h(\tau,y). \tag{54}$$

We make the coordinate transformation

$$\tau,s,y\to\tau,\sigma,y,\quad \sigma=s-h(\tau,y), \tag{55}$$

and examine Eqs. (53) in this edge-fixed coordinate system.

We seek a solution to Eqn. (53a) in $\sigma\neq 0$ in the form

$$\theta=\Phi_s(\sigma;\varepsilon)+\Phi'(\sigma,y,\tau;\varepsilon)=\Phi_s+\sqrt{\varepsilon}\,\Phi'_1(\sigma,y,\tau)+\varepsilon\sqrt{\varepsilon}\,\Phi'_3+\cdots \tag{56}$$

where Φ_s is the steady solution that we have already described (with the substitution $s\to\sigma$), and the other terms are perturbations. At the same time we write

$$h(y,\tau;\varepsilon)=\sqrt{\varepsilon}H(y,\tau). \tag{57}$$

Thus

$$\Phi'_1=0 \text{ in } \sigma>0 \tag{58}$$

and

$$\frac{\partial\Phi'_1}{\partial\tau}+V\frac{\partial\Phi'_1}{\partial\sigma}-\frac{\partial^2\Phi'_1}{\partial\sigma^2}-\frac{\partial^2\Phi'_1}{\partial y^2}+\Phi'_1=(H_\tau-H_{yy})\frac{d\Phi_0}{d\sigma}\quad \text{in } \sigma<0. \tag{59}$$

$O(\sqrt{\varepsilon})$ perturbations are not admissible within the flame edge so that the

boundary conditions for Eqs. (59) are

$$\underline{\sigma \to -\infty} \quad \Phi_1' \to 0, \quad \underline{\sigma = 0-} \quad \Phi_1' = 0. \tag{60}$$

We carry out a modal analysis in which the perturbations are proportional to $e^{\lambda\tau + iky}$, and then the solution of Eqs. (59), (60) is

$$\Phi_1{}' = H(1-\theta_w)\alpha_1 (e^{\alpha_1\sigma} - e^{\beta_1\sigma}), \sigma < O \tag{61a}$$

where

$$\beta_1 = \frac{1}{2}(V + \sqrt{V^2 + 4(\lambda + k^2 + 1)}). \tag{61b}$$

A perturbation equation valid everywhere can be constructed by eliminating $\tilde{\Omega}$ between Eqs. (53) and perturbing the resulting equation. Then if

$$J' = \frac{C_p T_a}{Q}\Phi' + Z', \quad J_s = \frac{C_p T_a}{Q}\Phi_s + Z_s, \tag{62}$$

where Z' is the unsteady perturbation in Y, we have

$$\frac{\partial J'}{\partial \tau} + V\frac{\partial J'}{\partial \sigma} + J' - \frac{\partial^2 J'}{\partial \sigma^2} - \frac{\partial^2 J'}{\partial y^2} + \varepsilon l \frac{\partial Z'}{\partial \tau} + \varepsilon l V \frac{\partial Z'}{\partial \tau} + \varepsilon C_{3_2} Z'$$

$$- \sqrt{\varepsilon}(H_\tau - H_{yy})\frac{dJ_s}{d\sigma} - \varepsilon\sqrt{\varepsilon}\, l\, H_\tau \frac{dZ_s}{d\sigma} = 0. \tag{63}$$

Corresponding to (56) we have

$$Y = Z_s + Z' = Z_s + \sqrt{\varepsilon} Z_1' + \varepsilon\sqrt{\varepsilon} Z_3' + \cdots, \tag{64a}$$

$$J' = \sqrt{\varepsilon} J_1' + \varepsilon\sqrt{\varepsilon} J_3' + \cdots, \tag{64b}$$

and, consistent with (63), we impose the constraint

$$J_1' = \frac{C_p T_a}{Q}\Phi_1' + Z_1' = 0. \tag{65}$$

Then the $O(\varepsilon\sqrt{\varepsilon})$ terms of Eq. (63) are

$$\frac{\partial J_3'}{\partial \tau} + V\frac{\partial J_3'}{\partial \sigma} + J_3' - \frac{\partial^2 J_3'}{\partial \sigma^2} - \frac{\partial^2 J_3'}{\partial y^2} + l\frac{\partial Z_1'}{\partial \tau} + lV\frac{\partial Z_1'}{\partial \sigma} + C_{3_2} Z_1'$$

$$-(H_\tau - H_{yy})\frac{d\Psi_2}{d\sigma} - lH_\tau \frac{dZ_0}{d\sigma} = 0, \tag{66}$$

where Ψ_2 is the steady-state function defined by Eqs. (50), (51), and could also be labeled J_{s_2}. J_3' vanishes at $\sigma = \pm\infty$ and we wish to calculate its value at $\sigma = 0$ for use in the flame-edge analysis.

To this end, we deduce from (66) that in

$$\underline{\sigma > 0} \quad J_3' = K_+ e^{\beta_2 \sigma} \tag{67a}$$

where

$$\beta_2 = \frac{1}{2}(V - \sqrt{V^2 + 4(\lambda + k^2 + 1)}); \tag{67b}$$

and in

$$\underline{\sigma < 0} \quad J_3' = K_- e^{\beta_1 \sigma} + \frac{A_1 e^{\alpha_1 \sigma}}{(\lambda + k^2)} + A_2 e^{\alpha_1 \sigma}\left(\frac{2\alpha_1 - V}{\lambda + k^2} + \sigma\right) + \frac{A_3}{(V - 2\beta_1)}\sigma e^{\beta_1 \sigma}, \tag{68a}$$

where

$$A_1 = \frac{C_p T_a}{Q} H(1 - \theta_w)\frac{lV}{2}\sqrt{V^2 + 4}(V + \sqrt{V^2 + 4}), \tag{68b}$$

$$A_2 = -\frac{C_p T_a}{Q} H(1 - \theta_w)\frac{lV}{2}(V + \sqrt{V^2 + 4}), \tag{68c}$$

$$A_3 = -\frac{C_p T_a}{Q} H(1 - \theta_w)\, lV\left\{1 + \frac{1}{2}\frac{\lambda}{V}(V + \sqrt{V^2 + 4})\right.$$

$$\left. + \frac{1}{4}(V + \sqrt{V^2 + 4})(V + \sqrt{V^2 + 4(1 + k^2)})\right\}. \tag{68d}$$

The constants $K_{\pm}$ are determined by the requirement that J_3' and its first derivative are continuous at $\sigma = 0$, whence

$$J_3'(0)(\beta_1 - \beta_2) = \frac{A_1(\beta_1 - \alpha_1)}{(\lambda + k^2)} + \frac{A_2(2\alpha_1 - V)(\beta_1 - \alpha_1)}{(\lambda + k^2)} - A_2 - \frac{A_3}{(V - 2\beta_1)}. \quad (69)$$

$J_3'(0)$ is the value of $(C_p T_a/Q)\Phi_3' + Z_3'$ everywhere within the flame-edge structure.

Perturbations in $\sigma > 0$

Behind the flame-edge, deviations from the Burke-Schumann limit are of the form

$$(\theta - 1) = \varepsilon\sqrt{\varepsilon}\left(-\frac{1}{\sqrt{D_1}} + \Phi_3'\right) + \cdots, \quad (70a)$$

$$(X - X_a) = \varepsilon\sqrt{\varepsilon}\left(\frac{C_p T_a}{Q}\frac{1}{\sqrt{D_1}} - \frac{C_p T_a}{Q}\Phi_3'\right) + \cdots, \quad (70b)$$

$$(Y - Y_a) = \varepsilon\sqrt{\varepsilon}\left(\frac{C_p T_a}{Q}\frac{1}{\sqrt{D_1}} + Z_3'\right) + \cdots, \quad (70c)$$

whence the perturbation reaction term is

$$\bar{\Omega}' = \bar{B}\varepsilon^3 \frac{C_p T_a}{Q} \cdot \frac{1}{\sqrt{D_1}}\left(-\frac{C_p T_a}{Q}\Phi_3' + Z_3'\right) + \cdots. \quad (71)$$

This is an $O(1)$ term and there is nothing to balance it, so that

$$Z_3' - \frac{C_p T_a}{Q}\Phi_3' = 0 \text{ in } \sigma > 0. \quad (72)$$

It follows that

$$\underline{\text{at } \sigma = 0+} \quad \Phi_3' = \frac{Q}{2C_p T_a} J_3'(0). \quad (73)$$

This is the perturbation flame temperature, a boundary condition to be imposed on the perturbed flame-edge structure, to which we now turn our attention.

Perturbed Flame-Edge Structure

Within the flame-edge we seek solutions that depend on $\xi = \sigma/\varepsilon$ in the form

$$\theta = \theta_s + \varepsilon\sqrt{\varepsilon}\,\theta'_3 + \cdots, \quad Y = Y_s + \varepsilon\sqrt{\varepsilon}\,Y'_3 + \cdots \tag{74}$$

whence

$$-\frac{d^2\theta_3}{d\xi^2} = \frac{Q}{C_pT_a}\frac{d^2Y'_3}{d\xi^2} = \bar{B}\varepsilon^3 e^{\theta_{s_2}}\left[\frac{C_pT_a}{Q}\theta^2_{s_2}\theta'_3 - \theta_{s_2}Y'_3 + \frac{C_pT_a}{Q}\theta_{s_2}\theta'_3\right]. \tag{75}$$

Since

$$\frac{C_pT_a}{Q}\theta'_3 + Y'_3 = J'_3(0), \tag{76}$$

(specified by Eq. (69)) this defines an equation for θ'_3 which is to be solved subject to the following boundary conditions:

$$\underline{\xi \to +\infty} \quad \theta'_3 \to \frac{Q}{2C_pT_a}J'_3(0) \tag{77}$$

(matching with Eq. (73));

$$\underline{\xi \to -\infty} \quad \frac{d\theta'_3}{d\xi} \to H(1-\theta_W)\alpha_1(\alpha_1 - \beta_1) \tag{78}$$

(matching with Eq. (61a)).

It is the solution of this two-point boundary-value problem that determines the dispersion relation governing the stability of the system.

It is helpful to rescale the problem by writing

$$\theta'_3 = \frac{Q}{-2C_pT_a}J'_3(0)\,\phi \tag{79}$$

whence

$$\frac{d^2\phi}{d\xi^2} = \bar{B}\varepsilon^3 \frac{C_p T_a}{Q} e^{\theta_{s_2}} [-\theta_{s_2}^2 \phi - 2\theta_{s_2} - 2\theta_{s_2} \phi] \tag{80a}$$

$$\underline{\xi \to +\infty} \quad \phi \to -1, \quad \underline{\xi \to -\infty} \quad \frac{d\phi}{d\xi} \to -\frac{2C_p T_a}{Q J_3'(0)} \mathrm{H}(1-\theta_w)\alpha_1(\alpha_1 - \beta_1) \tag{80b,c}$$

We define the functions u, v, f by

$$u = \frac{d\theta_{s_2}}{d\xi}, \; v = \frac{d\theta_{s_2}}{d\xi} \int_0^\xi \frac{d\xi}{[\mathrm{d}\theta_{s_2}/\mathrm{d}\xi]^2}, \; f = -2\bar{B}\varepsilon^3 \frac{C_p T_a}{Q} \theta_{s_2} e^{\theta}_{s_2} \tag{81}$$

and then the solution of Eq. (80a) is

$$\phi = K_1 u - u \int_0^\xi v f d\xi + v \int_{-\infty}^\xi u f d\xi \tag{82}$$

where K_1 is an undetermined constant. Note that, as $\xi \to \infty$,

$$u \propto 1/\xi^3, \quad v \propto \xi^4, \quad f \propto 1/\xi^2$$

so that ϕ approaches a constant at infinity and it is easy to show that this is (-1), as required.

Upon differentiating (82) we find,

$$\underline{\xi \to -\infty} \quad \frac{d\phi}{d\xi} \to \frac{-1}{d\theta_{s_2}/d\xi(-\infty)} \int_{-\infty}^\infty u f d\xi = -\sqrt{\varepsilon^3 \bar{B} \frac{C_p T_a}{Q}}, \tag{83}$$

and when this is equated to (80c) the dispersion relation is derived:

$$\begin{aligned} &(\sqrt{V^2+4} - \sqrt{V^2 + 4(\lambda + \mathrm{k}^2 + 1)}) \; (V^2 + 4(\lambda + 1 + k^2)) \\ &= (1-\theta_w) l \frac{V}{8} (\sqrt{V^2+4} + V) \; \sqrt{V^2 + 4(\lambda + 1 + k^2)} \\ &- (1-\theta_w) l \frac{1}{2} \left(V + \left(\frac{1}{2}\lambda + \frac{1}{4} V^2 \right) (V + \sqrt{V^2+4}) \right). \end{aligned} \tag{84}$$

This is a cubic in $\sqrt{V^2+4(\lambda+k^2+1)}$ and determines the gorwth rate λ as a function of k, V, and $(1-\theta_w)l$.

STABILITY RESULTS

It is convenient to describe the stability boundaries in the wave-number, Lewis-number plane. If we assume that θ_w is small compared to 1 and that $\varepsilon=\frac{1}{16}$, then

$$Le_Y \simeq 1+\frac{1}{16}(1-\theta_w)l. \tag{85}$$

The significant values of Le_Y that we shall identify are then not particularly close to 1 (an ingredient of the asymptotic treatment) but similar results for deflagrations suggest that this will not lead to false qualitative conclusions, or false order-of-magnitude conclusions. The 'robustness' of the NEF formulation for deflagrations, i.e. its reliability in describing subtle, complex qualitative behaviour, is well established.

Figure 8 shows the stability boundaries for $Le_Y<1$ ($l<0$). λ vansihes on each curve, which separates an unstable region on the left from a stable region on the right. When $V\to\infty$ (k fixed) the boundary is located at $(1-\theta_w)l=-4$ ($Le_Y\simeq 0.75$) and as V is decreased the boundary moves to the left. It approaches $-\infty$ as $V\to 0$, and there is no instability for $V\leqslant 0$. By analogy with deflagrations we expect that the instability will generate cellular structures. (Compare the curves in Figure 8 with Figure 5.3 in Buckmaster and Ludford (1983)).

Figure 9 shows the stability boundaries for $Le_Y>1$ ($l>0$). In general only the real part of λ vanishes on each curve, which separates a stable region on the left from an unstable region on the right. When $V=0$ there is instability at $k=0$ for $(1-\theta_w)l>8$ ($Le_Y\gtrsim 1.5$). λ vanishes when $V=0$, $k=0$, $(1-\theta_w)l=8$, but an increase in k introduces oscillations into the neutrally-stable mode. The frequency vanishes when $k=0$ for all of the curves shown in Figure 9 except for $V=3$, for which Im $(\lambda)=3.55$. Thus oscillations are a characteristic of the instability but it seems likely that if $V=0, k=0$ (for example) an infinite-period Hopf bifurcation analysis would be necessary to calculate the frequency as a function of the small parameter $(1-\theta_w)l-8$. Figure 9 should also be compared with Figure 5.3 in Buckmaster and Ludford (1983).

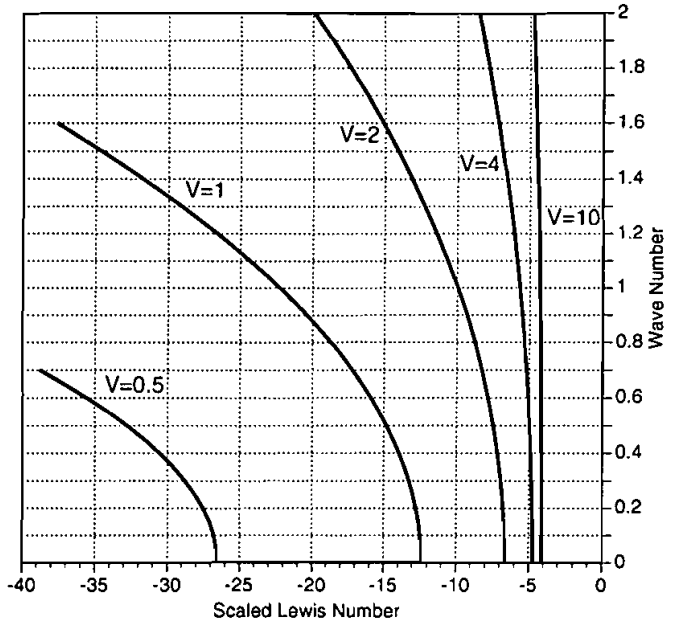

FIGURE 8 Stability boundaries in the k-$(1-\theta_w)\,l$ plane, $Le_Y < 1$.

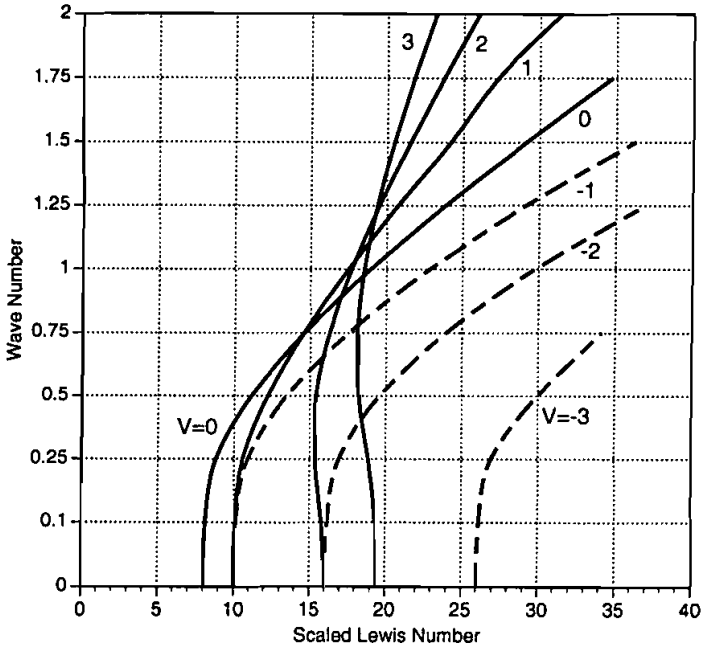

FIGURE 9 Stability boundaries in the k-$(1-\theta_w)\,l$ plane, $Le_Y > 1$.

CONCLUDING REMARKS

In this exploratory study we have examined a one-dimensional model designed to contain some of the important physics that control edge-flames. It exhibits some of the characteristics of deflagrations, specifically a preheat zone containing the mixture, terminated by an intense reaction zone (the flame-edge). And it exhibits some of the characteristics of diffusion flames in that, behind the edge, heat generated by residual reaction is removed by a term that represents losses to side boundaries, and the fuel and oxygen necessary to sustain the reaction are supplied by appropriate 'side-terms'.

How well such a model can predict the dynamics of edge-flames, and how robust it is, are questions that can only be answered by further studies, analytical, numerical, and experimental. But the present results suggest that cellular structures are possible in advancing edges (but not in stationary or retreating ones) when the Lewis number is small; and pulsations and travelling waves are possible for edges travelling with modest speed (positive or negative) when the Lewis number is large.

Cellular structures and pulsations have been observed experimentally in edge-flames (see the Introduction), but it must be noted that there are important differences between the experimental configurations and the model as presently defined. Strong premixing is a characteristic of the model ($X \to X_w$, $Y \to Y_w$ as $z \to -\infty$) but in the candle configuration there is no fuel supply far ahead of the edge. To account for this it would be necessary, amongst other things, for Y_w to be a function of T, since this provides the evaporative force.

The flame in the Kirkby-Schmitz apparatus and the burner flame are anchored rather than freely propagating, so that here also the model needs to be modified if it is to more accurately reflect these physical situations. (An interesting example of an anchored flame is reported by Pellett, Northam and Wilson (1991), who observe holes in lean hydrogen/air counter flow flames. The edge of each hole, symmetrically disposed, maintains a fixed position in the radial flow).

Clearly there are a number of problems that can be explored using one-dimensional models similar to the one described here, and there is promise that useful physical insights can be gained. The one-dimensional approach clearly has an advantage over two-dimensional strategies that require formidable numerical calculations (e.g. Kioni *et al.* 1993)).

Acknowledgements

This work was supported by AFOSR and by the NASA-Lewis Research Center. I am grateful to Rodney Weber whose fine presentation on non-adiabatic thermal waves (*loc. cit*) at the US-Japan combustion workshop held at Kapaa, Kauai in 1994 planted one of the seeds that led to the work described here; and to Howard Ross whose candle-flame video planted another.

References

Buckmaster, J. D. and Ludford, G. S. S. (1983). *Lectures on Mathematical Combustion*, CBMS-NSF Regional Conference Series in Applied Mathematics, No. 43, SIAM, Philadelphia, PA.

Chan, W. Y. and T'ien, J. S. (1978). *Combust. Sci. and Tech.*, **18**, 139.

Chen, R., Bradley, G., and Ronney, P. D. (1992). Proc. 24th (Intl.) Symp. on Combustion, The Combustion Institute, Pittsburgh, PA, pp. 213–221.

Dietrich, D. L., Ross, H. D. and T'ien, J. S. (1994). *Candle flames in non-buoyant and weakly buoyant atmospheres*, AIAA 34th Aerospace Sciences Meeting, AIAA-94–0429.

Dold, J. W., Hartley, L. J., and Green, D. (1991). in *Dynamical Issues in Combustion Theory*, IMA Volumes in Mathematics and its Applications (P. C. Fife, A. Liñán, and F. A. Williams, eds.), Springer, New York, pp. 83–105.

Grindrod, P. (1991). *Patterns and Waves*, Clarendon Press, Oxford.

Kioni, P. N., Rogg, B., Bray, K. N. C., and Liñán, A. (1993). Combust. and Flame, **95**, pp. 276–290.

Pellett, G. L., Northam, G. B., and Wilson, L. G. (1991). *Counter flow diffusion flames of hydrogen, and hydrogen plus methane, ethylene, propane, and silane vs. air:Strain rates at extinction*, AIAA–91–0370.

Spalding, D. B. (1957). Proc. Roy. Soc. London, **240 A**, 83–100.

Weber, R. O., Mercer, G. N., Gray, B. F. and Watt, S. D. (1995) in *Modeling in Combustion Science*, (eds. John Buckmaster and Tadao Takeno), Lecture Notes in Physics 449, Springer-Verlag, Berlin, pp. 285–295.